Chapter 3

Folic Acid Modified Mesoporous Silica Nanoparticles for Cellular and Nuclear Targeted Drug Delivery

Abstract. Site-specific stimuli responsive nanomaterials are an important breakthrough for the improvement of modern therapies in nanomedicine. Mesoporous silica nanoparticles are good candidate for the development of targeted delivery system as their surface can be easily modified with functional groups in order to achieve controlled and specific release. We designed a drug delivery system based on mesoporous silica nanoparticles modified with folic acid as a specific targeting moiety. The functionalization forms a nanovalve system in which the surface is modified with an aliphatic chain. This stalk tethers a cyclodextrin with the specific role to prevent undesired release of the cargo. To avoid any movement of the cyclodextrin the folic acid is placed at the end of the chain. The release kinetics were investigated with UV/VIS spectroscopy and cellular uptake was extensively studied using flow cytometry. Through this study we demonstrated the biocompatibility of folic acid modified MSNs and the effective release of an encapsulated anticancer drug using TUNEL and Western Blot assays.

3.1 Introduction

Site-specific stimuli delivery systems are attractive materials as drug delivery system (DDS) for the treatment of cancer disease in which the ultimate goal is the release of significant amount of drug in selected areas without damaging surrounding healthy cells.[1-3] Therefore the drug carrier must posses a number of properties such as biocompatibility with a living environment; high loading capacity of the drug; prevention of any premature release, and the ability to target specific cancer cells and controlled release. [2, 4] In the last decade, a wide variety of DDS were explored based upon dendrimers, hydrogels, liposomes, and inorganic nanoparticles.[5-10] However, mesoporous inorganic nanomaterials represent a good candidate for drug delivery as they preserve the payload from the metabolism and the immune response for a longer period of time. Therefore, the distribution of the nanocarrier in all the districts of the organism reaching the targeted site and releasing a significant concentration of drug can be achieved.[2, 11-13] In order to accomplish targeting and tunable release inorganic nanoparticles have undergone to surface modification.[14]

Mesoporous silica nanoparticles (MSNs) are actively studied materials for drug delivery because of their fascinating properties.[15] These nanomaterials were evaluated *in vivo* and high biocompatibility was observed. Moreover, the pore size can be varied thereby allowing the loading of guest molecules with different molecular weight and variable steric hindrance. The organic modification of the nanocarrier surface transforms the nanomaterial into a "smart" drug release device where the valves have three important functions: to prevent any premature release, to deliver the payload upon specific stimuli in order to avoid any side effect, and to target the system towards a specific cell type.[16-20]

In order to prevent aggregation in aqueous media hydrophilic valves have been designed composed of peptides,[21] antibodies,[22, 23] DNA/dendrimers complexes and lipid bilayers.[23] In this paper we studied a new stimuli-responsive material based on silica mesoporous nanoparticles capped with rotaxane valves and a folic acid head group.

The nanovalve system consists of a monolayer of mechanically interlocked molecules in the form of the rotaxane composed of: a linear stalk anchoring the rotaxane on the surface, a gating ring which encircles it and locks the cargo in the mesopores, and a stopper located at the end of the linker connected to it with a cleavable bond.[15]

In this chapter, the so-called rotaxane nanovalves are activated by esterase enzymes while the targeting moiety folic acid is an integral part of the valve system. Folic acid, the

soluble form of Vitamin B, targets tumors in similar manner of monoclonal antibodies: since folate receptors (FRs) are overexpressed in more than 40% of human tumors,[24] while generally absent in healthy cells.[25]

3.2 Results and Discussion

3.2.1 Design and synthesis of the folic acid modified nanovalve

We previously used silica modified nanoparticles with folic acid in order to increase the selectivity towards cancer cells. However in these studies the folic acid was not a part of a nanovalve system.[26-32]

The rotaxane structures locks the guest molecules in the pores while preventing any premature leakage. The folic acid moiety is an integrated part of the rotaxane structure (**Scheme 1**). Nanoparticles loaded with the anticancer drug camptothecin (CPT) were evaluated as a drug release system in cell cultures and its effect on the apoptosis mechanism of the cells was studied with Western Blot and TUNEL staining assays.

Folic acid modified mesoporous silica nanoparticles (FAMSNs) were synthesized from tetraethyl orthosilicate (TEOS) using CTAB as a surfactant template agent.[2, 33-35] Scanning electron microscopy (SEM) showed that the particles were spherical with an average diameter of 200 nm. The surfactant was subsequently removed as described in **Chapter 2** and the successful reaction was proven by Fourier Transform Infra Red spectroscopy. The nanoparticles were analyzed with TEM in order to confirm the presence of nanopores as already shown in **Chapter 2**.

For the construction of the nanovalve at the silica nanoparticles the folic acid was modified with ethanolamine (**2**) and coupled with pentynoic acid for the introduction of an alkyne moiety (**3**) as shown in **Scheme 1**.[36-38] Next, the MSNs modified with an azide terminus (**4**) were modified with the folic acid moiety using a copper(I)-catalyzed click reaction.

3.2.2 Study of the release kinetics

The prevention of uncontrolled release of therapeutic molecules before reaching the desired targeted cell is an important property of a drug delivery system. Therefore we investigated the release of fluorescein, a model compound for our kinetic studies. The nanoparticles were loaded with 5 mM solution of fluorescein overnight and capped with the rotaxane and the folic acid moiety. Next, the nanosystem was washed three times with phosphate buffer solution (PBS) to remove excess of fluorescein.

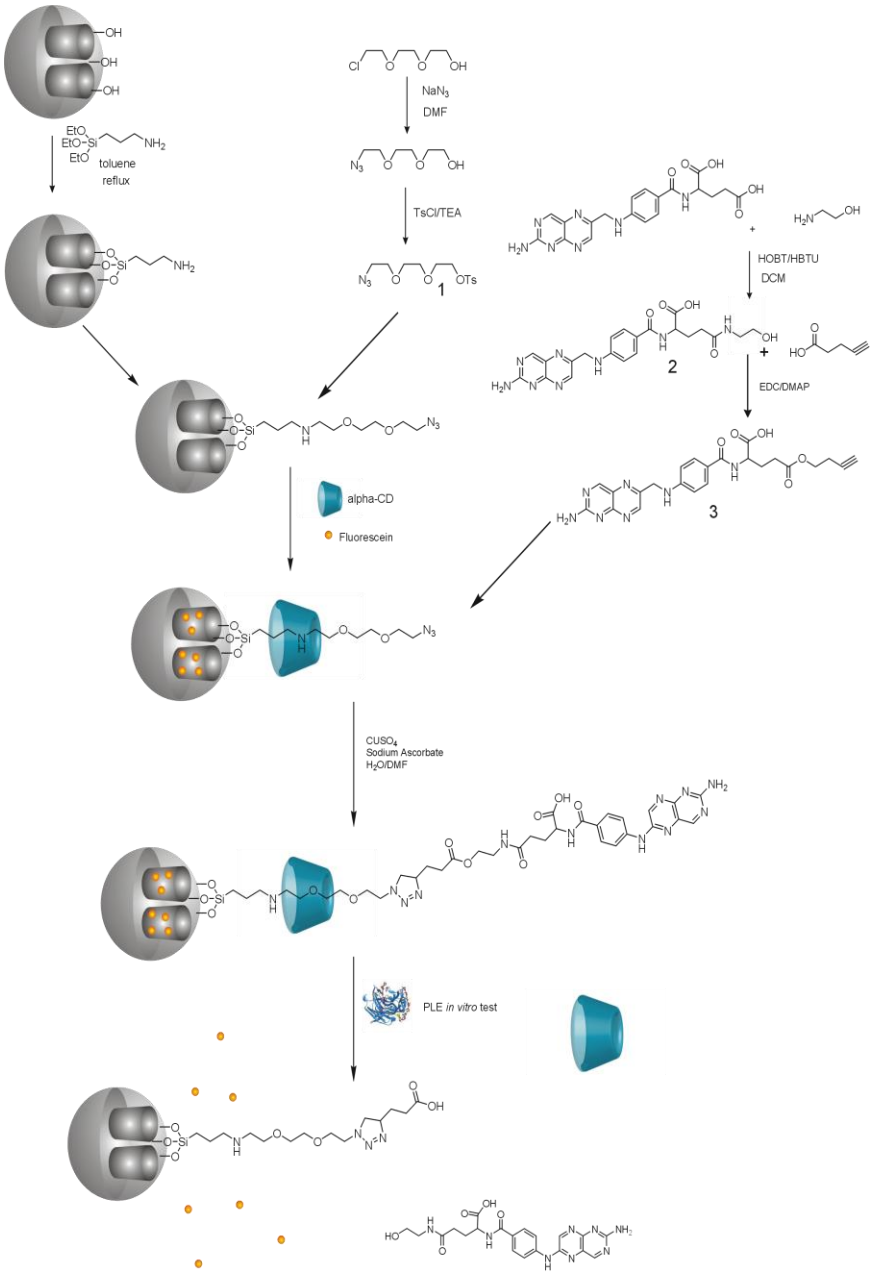

Scheme 1. Synthesis of the Folic Acid Silica Nanoparticles (FAMSNs), the particles are loaded with fluorescein which is released upon bioactivation of the valve towards Porcine Liver Esterase (PLE).

Typically FAMSNs contained approximately 4.6 nmol of fluorescein per mg of nanoparticles. Next, the release was investigated *in vitro* in the presence of porcine liver esterase (PLE). Interestingly the release showed a lagtime of 30 min and we hypothesize that the cyclodextrin acts as a steric shield for the ester bond from the hydrolization reaction, which is different compared to earlier work.[20] In the absence of esterase, the rotaxane structures prevent undesired release of dye showing its effectiveness as a valve system (**Figure 1**).

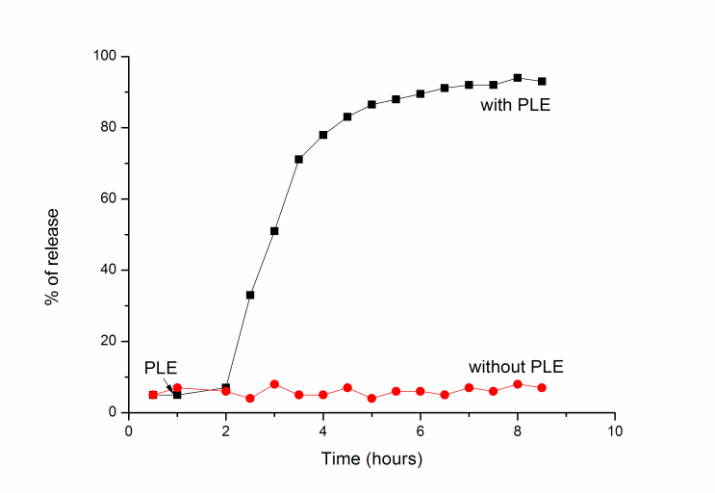

Figure 1. Controlled release of fluorescein in the presence (■) and absence (●) of 0.12 mL Porcine Liver Esterase (PLE) with a concentration of 10 mg mL^{-1} in 3.2 M $(NH_4)_2SO_4$. All the data are expressed as a mean values ± the standard deviation (SD).

3.2.3 Hydrodynamic radius studies

For efficient drug delivery into cells it is necessary that the nanoparticles do not cluster in media as they will lower the cellular uptake. Hence it is important to create a hydrophilic surface and avoid any undesired interactions between the particles. The surface functionalization achieves this goal, because the folic acid moiety gives hydrophilic properties to the nanoparticles and the cyclodextrine prevents aggregation in media. As shown in a previous study[21] we investigate the importance of the cyclodextrine (α-CD) tethered on an aliphatic stalk when nanoparticles are dispersed in aqueous solutions. The shielding action of the α-CD prevents inter-particle aggregation; thus clustering in physiological media is minimized.

Dynamic light scattering (DLS) measurement was performed in order to understand the purpose of the organic functionalization. Silica nanoparticles have the tendency to aggregate in buffered media and therefore strategies have been developed in order to prevent this phenomenon.[14, 17, 27] One of the most exploited methods is the pegylation of the external surface which preclude clustering effects and without any precipitation in fetal serum. [39-41] In our case, the organic surface functionalization also precludes aggregation and at the same time it functions as an esterase-activated snap-top drug delivery system. The hydrodynamic radius of unmodified MSNs in PBS buffer indeed indicated clustering of the particles while FAMSNs showed to be monomeric (Rh= 517 nm and 196 nm respectively) (**Figure 2**). Thus the presence of this rotaxane structure including the folic acid moiety, prevents clustering of the particles effectively and the observed diameter correspond well with the average size obtained by SEM (approximately 200 nm).

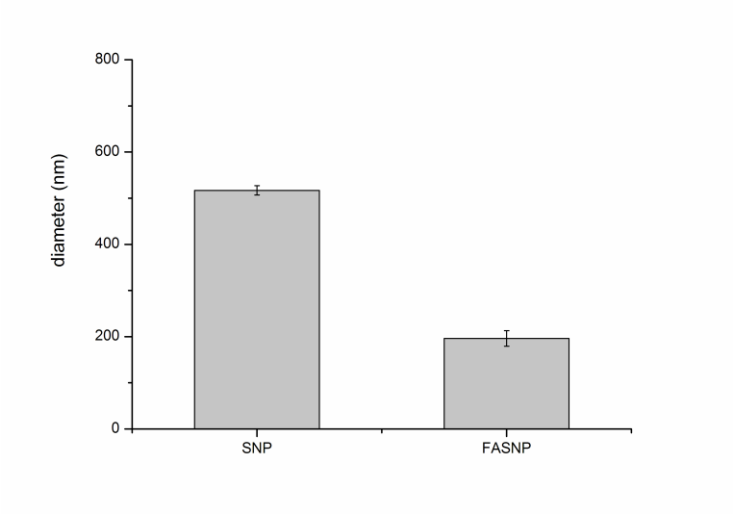

Figure 2. Hydrodynamic diameter of mesoporous silica nanoparticles (MSN) and Folic Acid Silica Nanoparticles (FAMSNs) determined with dynamic light scattering. the analysis has been done in PBS buffer 1M (pH=7.24); MSN aggregates in buffer solution while FAMSNs have the tendency to remain separate and do not aggregate due to the effect of the surface functionalization.

3.2.4 Cellular uptake investigations and imaging

A homogenous suspension containing fluorescein-loaded FAMSNs (1 μg mL^{-1}) in PBS were incubated with U2Os cells for 1 hour in medium to study the cellular uptake and toxicity. The cells were washed to remove any cell membrane adhered FAMSNs and analyzed with confocal laser scanning microscopy. The nuclei of the cells were stained with 4',6-diamino-2-phenylindole (DAPI) and cell cytoskeleton was marked with phalloidine-Alexafluor 594. The cells showed to have green fluorescent nanoparticles in the cytoplasm revealing that the FAMSNs are taken up by the cancer cells. The presence of nanoparticles was observed in all the cultured cells analyzed.

The efficiency of FAMSNs uptake was quantified with flow cytometry as a function of time showing an increasing internalization of FAMSNs in cancer cells while in the control experiment unmodified MSNs did not show this trend (**Figure 3**). In approximately 90% of the U2Os cells endocytosis of FAMSNs was determined. Thus, the functionalization with folic acid positively influences the uptake of FAMSNs by cancer cells, indicating that the over expressed of folic acid receptors are involved in the cellular uptake (**Figure 3B1**, **B2** and **B3**).[24, 42, 43] Surprisingly FAMSNs were also observed in the nucleus of U2Os cancer cells (**Figure 3B3)**. Bozard and collaborators[44] studied the localization of folate receptors showing their presence in the nuclear membrane. Therefore, our findings confirm this study of Bozard since the FAMSNs are taken up in the nucleus using the receptor mediated mechanism. To prove our hypothesis we studied the cellular uptake of unmodified MSNs

with the same experimental conditions with laser confocal microscopy. In this study the nanoparticles were found only in the cytoplasm.

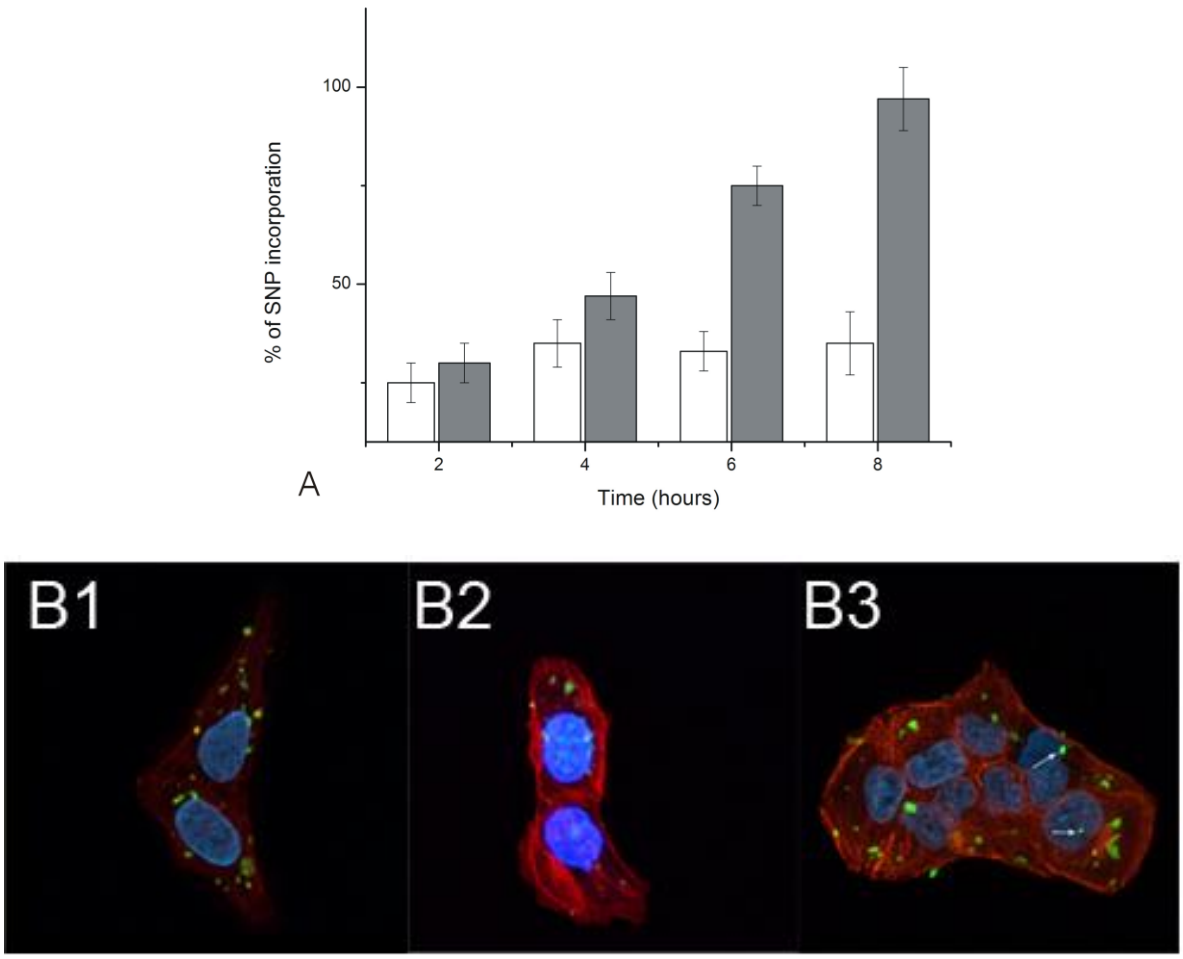

Figure 3. U2Os endocytosis experiment. (A) Graph representing the inclusion percentage of Folic Acid Silica Nanoparticles (FAMSNs, gray bars) versus unmodified mesoporous silica nanoparticles (white bars), due to surface functionalization the FAMSNs are selectively uptaken by cancer cells, while bare silica nanoparticles do not show this tendency. (B) Laser confocal microscopy of U2Os cells with FAMSNs (green); (B1) the white arrow indicates the presence of FAMSNs (green) in the nucleus (blue DAPI) and around the nuclear membrane while red fluorescence represent actin filaments of the cell cytoskeleton, (B2) U2Os cells with particles in the nucleus indicated by the white arrow.

3.2.5 Release of camptothecin in osteosarcoma cancer cells

The drug delivery of camptothecin (CPT) in human cancer cells leads to growth inhibition and cell death. However, CPT is hydrophobic thus the formulation and the delivery of this drug remains a challenge. Therefore the delivery of CPT using FAMSNs can increase the efficacy of this molecule preventing serious side effects as the compound is released only in the targeted cells. When a cancer cell enters the apoptosis pathway there is an activation of several mechanisms which lead the cell to a programmed death.

Activation of specific enzymes as caspase-3 and fragmentation of nuclear DNA are the most investigated pathways.[45-48]

To study the effective release of the anticancer drug CPT from the FAMSNs into the cytoplasm was investigated with Terminal deoxynocleotidyl transferase dUTP Nick End Labeling (TUNEL) assay and Western blot analysis.

CPT-loaded FAMSNs were incubated with U2Os at 37 °C and then fixated after 30 min, 60, 180 and 240 min. Next, we studied the effect of released CPT on the cell with the TUNEL assay. In **Figure 4A**, **B** and **C**, laser confocal images are reported of samples fixated after 60, 180 and 240 min. TUNEL positive cells bear green fluorescence in the nuclear region due to selective interaction of the labeled nick end with fragmented DNA. We determined the percentage of cellular death (TUNEL positive cells) versus time of incubation and observed that 90% of the cells were positive after 240 min. Thus folic acid modified nanocarriers after being uptaken by cancer cells, release their payload in an effective manner as confirmed by DNA fragmentation of TUNEL positive cells. We also investigated whether the MSNs and FAMSNs showed any toxicity. **Figure 4E** shows the positive TUNEL cells after incubation with MSNs (control), a solution of 5 mM of CPT in DMSO[14], FAMSNs and CPT loaded FAMSNs. MSNs and FAMSNs showed biocompatibility properties when incubated with U2Os cells and a low cytoxicity was observed. The effect on the apoptosis of a solution in DMSO of the anticancer drug CPT was observed as approximately 50% of cultured cells were found positive. However 93% were found positive when exposed to CPT-FAMSNs nanoparticles. This result is very important as the calculated amount of CPT released by the suspension of nanoparticles used for the assay was 0.4 nmol of CPT per µg of FAMSNs. Thus significantly lower than the amount previously used. Therefore, loading nanoparticles with CPT increase significantly the efficacy of this drug, as it is delivered directly in the cellular environment. Moreover the prevention of any premature release allows the delivery of significant concentration of CPT at targeted site.

To investigate the cellular release of CPT loaded FAMSNs a Western Blot was also performed. This analysis allows the detection of the activated capsase-3 enzyme specific for apoptotic pathways. After 240 min cells treated with FAMSNs CPT loaded were analyzed confirming our hypothesis that CPT was effectively released by the nanocarrier. Any activation was detected in the control experiment in which unloaded nanoparticles were used.

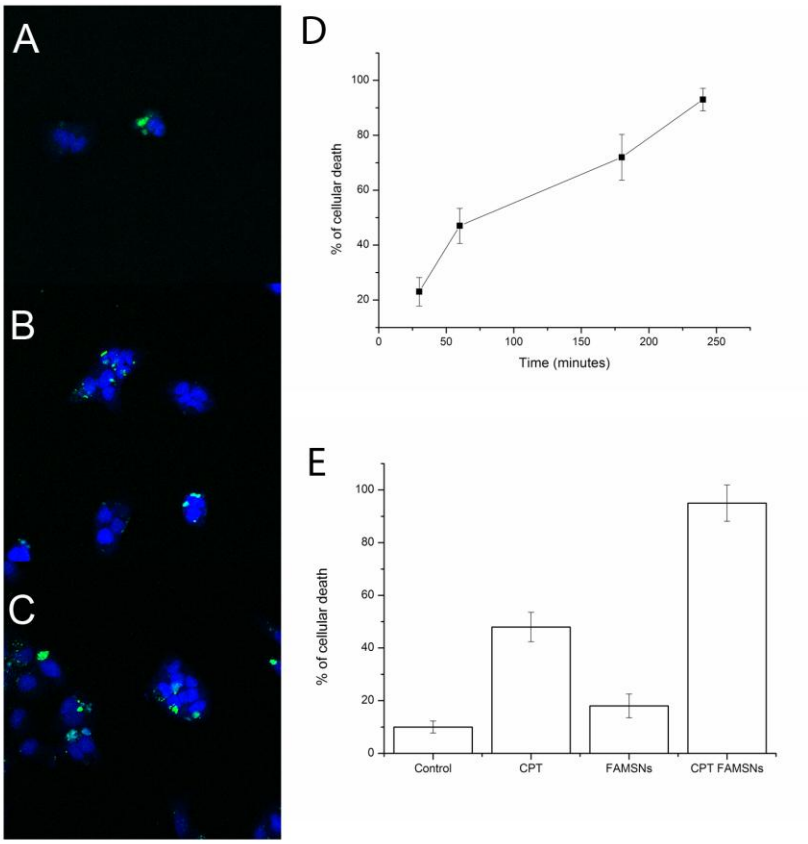

Figure 4. TUNEL staining assay in U2Os cells. U2Os were incubated with FAMSNs loaded with CPT and they were analyzed with laser confocal microscope. Positive apoptotic cells have green fluorescent nuclei, while not apoptotic cells have blue (DAPI) nuclei. (A) Laser confocal image after 1 hour, (B) after 3 hours and (C) after 4 hours. (D) Amount of positive TUNEL cells in the time. After 4 hours of incubation approximately the 90% of U2Os observed was found apoptotic. (E) TUNEL assay performed with MSNs (control), FAMSNs, a solution in DMSO of CPT and FAMSNs loaded with CPT. MSNs and FAMSNs have shown low cytotoxicity very similar to normal turnover of a cell culture. The 50% of U2Os cells were found dead after exposure of CPT solution in DMSO, while the 93% of cells were found positive to TUNEL after exposure to FAMSNs-CPT loaded. Thus the nanoparticles vehiculate the drug directly in the cytoplasm releasing an effective amount of drug in the cytoplasm.

3.3 Conclusions

In summary, we designed a site specific drug delivery system using the so-called nanovalve concept. FAMSNs release their cargo upon a biological stimulus (i. e. esterase) and no leakage was observed in the absence of this enzyme. Thus this system prevents significantly severe side effects due to unspecific release of drug. A lag time of approximately 30 min was observed due to the steric hindrance of the tethered rotaxane. Moreover, the cyclodextrin has a crucial role in preventing aggregation as shown by DLS experiment. Active internalization is observed when folic acid is a part of the surface functionalization of the nanocarrier as confirmed by flow cytometry studies. The FAMSNs

have demonstrated to be biocompatible as they do not induce apoptosis in U2Os cultured cells. This result was also confirmed by a TUNEL assay where the cytotoxicity was compared with unmodified MSNs. The release of CPT from the FAMSNs was detected and quantified as a function of time with TUNEL and Western Blot assays. Hence, the delivery of the anticancer drug led to the detected pharmacological effects as a significant concentration of compound was released in the cytoplasm of the cells.

At present, a large number of molecules in the pipeline of pharmaceutical companies have low water solubility and therefore some administration ways are precluded at all.[49] The employment of mesoporous silica nanoparticles to encapsulate hydrophilic anti-cancer drugs is one of the most promising strategies to deliver these compounds in living organisms. The ability to functionalize the silica surface with specific targeting molecules enhances the possibility to have successful therapies for cancer diseases and vaccine applications. Further work is necessary to establish these functionalized silica nanoparticles as a tool for selective and target release while minimizing cytotoxic side effects.

3.4 Experimental part

Synthesis of the nanoparticles. The synthesis of nanoparticles was performed accordingly with the procedure explained in **Chapter 2**. The characterization of the nanomaterial was execute as described in the same chapter.

Preparation of amine-modified mesoporous silica nanoparticles. To functionalize the surface of the particles, 100 mg of SNP was suspended in 10 mL of anhydrous toluene with 1 mmol (0.221 mg) of amino propyl triethoxysilane (APTES) and refluxed overnight in a inert atmosphere. The suspension was filtered and a white solid was obtained.

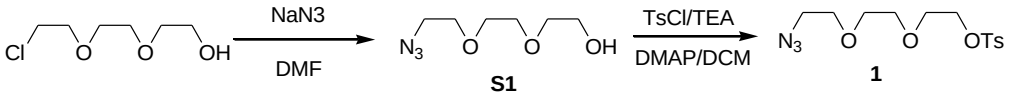

2-(2-(2-Azidoethoxy)ethoxy)ethanol (S1). A mixture of 2-(2-(2-azidoethoxy)ethoxy)ethanol (5.0 g, 30 mmol) and NaN_3 (3.0 g, 45 mmol) was dissolved in 100mL of DMF and stirred at 100 °C for 48 hours. The reaction mixture was then cooled to RT, filtered and the solvent was removed under vacuum to afford the product S1 (5.1 g, 97%) as a colourless oil. ^{1}H NMR ($CDCl_3$ δ) 1.5 (t, J=5.5 Hz 2H), 3.4 (m, 2H), 3.54 (m, 4H), 3.56 (m, 4H) 3.70 (t, J=6.0 Hz, 2H), 4.78 (m, 2H)

2-(2-(2-Azidoethoxy)ethoxy)ethyltoluensulfonate (1). A mixture of compound S1 (1.0 g 5.7 mmol), DMAP (80 mg, 0.66 mmol) and Et_3N (4.0g, 40 mmol) was dissolved in 150 mL of DCM and cooled

to 0 °C. Next, a solution of p-toluenesulfonyl chloride (4.77 g, 25 mmol) in 50 mL of DCM was added dropwise. The mixture was allowed to warm to RT and stirred for 18 hours. The solvent was removed under vacuum and the crude mixture was passed through a silica plug with EtOAc as eluent. Next, the EtOAc phase was washed with H_2O (2x50 mL) and with 50 mL of brine. The solvent was evaporated in order to give the compound 1 (yield 1.2 g, 83%) as a pale orange oil. ^{1}H NMR ($CDCl_3$ δ) 1.5 (t, J=5.5 Hz 2H), 2.43 (s, 3H), 3.4 (m, 2H), 3.54 (m, 4H), 3.56 (t, J=6.2 Hz 2H), 3.70 (m, 2H), 7.48 (m, 2H), 7.76 (m, 2H).

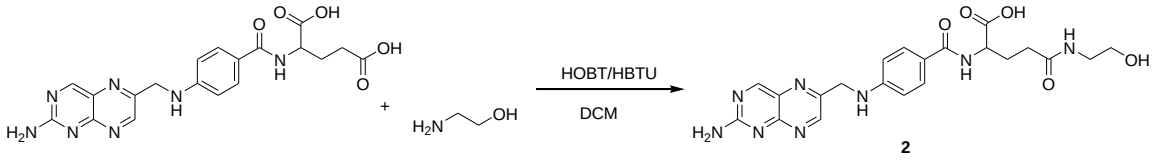

Folic Acid modification with ethanolamine. 0.3 g of folic acid (0.679 mmol) was dissolved in 50 mL of DCM cooled to 0 °C and 0.679 mmol (0.092 g) of HOBT, 1.0185 mmol (0.386 g) of HBTU and 0.339 mmol (0.021 mL) of ethanolamine were added. A clear solution was obtained and 1.358 mmol (0.237 mL) of DIPEA was added. The mixture was stirred overnight at room temperature.

After removal of the solvent the organic layer was washed with Milli-Q water (3x50 mL), with 30 mL of $NaHCO_3$ 2 M and with 30 mL of brine. The product was purified by silica gel column chromatography (DCM/MeOH 90:10 v/v), resulting in a yellow solid (**2**) with a yield of 76%. ^{1}H NMR ($CDCl_3$ δ) 2.10-2.18 (m, 4H), 3.39 (t, 2H, J=2.20Hz), 3.79 (t, 2H, J=2.23 Hz), 4.78 (s, 1H), 4.32 (m, 2H), 4.46 (s, 1H), 6.59-6.65 (m, 5H), 7.56 (m, 2H), 8.47 (s, 1H), 8.57 (s, 1H), 8.88 (s, 1H), 8.01 (s, 1H)

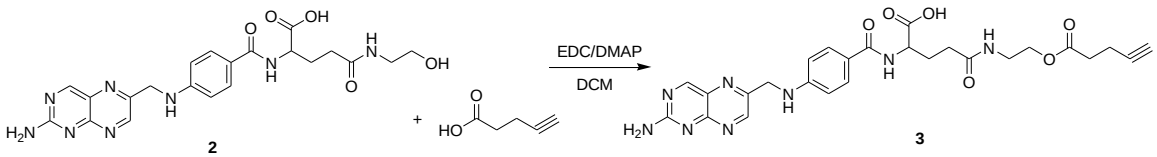

Folic acid pentynoic Acid Ester (3). A solution of pentynoic acid (67 mg, 0.675 mmol) and 1-ethyl-3-(3-dimethylaminopropyl)-carbodiimide (EDC) (172.3 mg, 0.9 mmol) in 10 mL of DCM was cooled to 0 °C before a solution of modified folic acid (**2**) (0.2 g, 0.45 mmol) in 30 mL of DCM was added. The reaction slowly warmed up to room temperature and was stirred for 2 hours before the addition of 4-(methyldiamino)pyridine (DMAP) (5.33 mg, 0.043 mmol). After 24 hours the mixture was poured into 50 mL of MilliQ water and washed with DCM (3x50 mL). The resulting organic layer was washed three times with 50 mL of Milli-Q water, $NaHCO_3$ (2 M, 30 mL) and brine (30 mL). The compound was purified by silica gel column chromatography (70:30 v/v Hexanes: Ethyl Acetate) providing a yellow crystalline compound (0.093 g, 43.3%). ^{1}H NMR ($CDCl_3$ δ) 1.82 (s, 1H), 2.10-2.18 (m, 4H), 2.42 (m, 4H), 3.48 (t, 2H J=3.87Hz) 4.34-4.50 (m, 5H), 6.57-6.62 (m, 3H), 7.56 (d, 2H J=5.27 Hz), 8.01 (s, 1H), 8.47 (s, 1H), 8.57 (s, 1H), 8.88 (s, 1H)

General procedure of the synthesis of FAMSNs snap-top system. 100 mg of amine-modified mesoporous silica nanoparticles were suspended in 10 mL of dry methanol and 1 mmol of 2-(2-(2-azidoethoxy)ethyl)ethylsulfonate (compound **1** in Supporting Information) and refluxed overnight, followed by filtration resulting in a white fine powder. Next, a mixture of the azide-functionalized nanoparticles (100

mg), fluorescein (10 mg, 0.031 mmol) and α-CD (480 mg, 0.493 mmol) were suspended in a mixture of 50:50 DMF and MilliQ water (20 mL) and stirred for 24 hours at 5 °C. Then 1 mmol of compound **2** (supporting Information) was added, followed by the addition of $CuSO_4$ (1.5 mg, 0.098 mmol) and ascorbic acid (4 mg, 0.019 mmol) and the mixture was stirred for 3 days at 5 °C. The nanoparticles were filtered and washed several times with MeOH and MilliQ water to remove the unreacted compound.

General procedure for preparation of CPT-loaded FAMSNs. A mixture containing 100 mg of the azide-functionalized nanoparticles and α-CD (480 mg, 0.493 mmol) were suspended in 10 mL of 50 mM solution CPT in DMSO and stirred for 24 hours at 5 °C. Then 1 mmol of compound **2** (see SI) was added, followed by the addition of $CuSO_4$ (1.5 mg, 0.098 mmol) and ascorbic acid (4 mg, 0.019 mmol). The suspension was stirred for other 3 days at 5 °C and after filtration the nanoparticles were collected and stored at 4 °C until further use.

General procedure for enzymatic activation of the snap-top system. A sample of fluorescein loaded nanoparticles (10 mg) was placed in the bottom corner of quarz cuvette and 1.2 mL of HEPES buffer solution (50 mM, pH=7.5) was added. A sample of pig liver esterase (PLE) solution (0.12 mL, 10 mg mL^{-1} in 3.2 M $(NH_4)_2SO_4$) was added and the absorption spectra was measured with UV-VIS Cary 5 Bio Varian spectrophotometer for 1 day. The release was calculated analysing the concentration of fluorescein in the supernatant at 500 nm, 92,300 M^{-1} cm^{-1}.

Particle size measurements. Hydrodynamic radii were measured with a DLS-Zetasizer, NanoSeries Malvern. 1 μg mL^{-1} of particles were suspended in 1 mL of PBS (pH=7.2) and sonicated for 2 hours the hydrodynamic radius was measured.

Cell culture. U2Os, osteosarcoma cancer cells were obtained from the American Tissue and Cell Collection: HB-96 and were maintained in Dulbecco's modified Eagle's medium (DMEM, GIBCO) supplemented with 10% of fetal calf serum Iron supplied, 2% of L-glutamine, 1% of penicillin and 1% of streptomycin. The cells were cultured at 37 °C with 5% of CO_2. The media were refreshed every two days, and the cells were passaged by trypsinization before reaching the confluence.

Fluorescence and confocal microscopy. In all experiments cancer cells were maintained in DMEM in a Lab-Tek chamber slide system (Nalgen Nunc International) and incubated with FAMSNs at the concentration of 100 μg mL^{-1} for 1 hour at the temperature of 37 °C with the 5 % of CO_2. The cell culture was then washed three times with DMEM in order to remove all the nanoparticles that did not enter the cells. To examine the localization of FAMSNs within the cells a laser scanning confocal microscopy was performed with a Carl Zeiss LSM 5 exciter microscope with excitation wavelength of 470 nm and emission wavelength 525 nm for fluorescein, 305 nm as excitation wavelength and emission at 470 nm for DAPI and Phalloidine-Alexafluor 568 the excitation wavelength was 578 nm and emission at the wavelength of 603 nm. The procedures for cell staining are described in the Supporting Information.

Alexafluor 568-Phalloidine staining procedure. U2Os cells were incubated in a 4 well chamber with FAMSNs overnight and then they were treated with the fixation buffer at room temperature for 10 min and rinsed for 10 min with a 1 mL of a solution of sodium borohydride in PHEM buffer (2 mg mL^{-1}). The wells were washed with 2 mL of PHEM buffer (3x15 min), and then with 2 mL BSA blocking buffer for 10 min.

Afterwards the solution was removed from the well and a 100 µL of the Phalloidin-Alexafluor 568 solution was added. The system was incubated for at least 30 min at room temperature in the dark.

The cells were incubated with 1 mL of BSA blocking buffer (4x20 min), and finally the solution was removed and replaced with 1 mL of MilliQ water. The samples were analyzed with laser confocal microscope.

Cell nucleus staining protocol. Cell nuclei were stained with DAPI purchased by Molecular Probes. 5 µL of concentrated DAPI in Milli-Q (stock solution 5 mg/mL) was diluted in 1 mL of DMEM and 500 µL of this solution was added to the well containing the U2Os cancer cells. After 20 min of incubation at 37 °C blue fluorescent nuclei were visualized with laser confocal microscope.

Flow cytometry. The cellular uptake of FAMSNs was monitored with flow cytometry; the discrimination between internalized FAMSNs and FAMSNs only adsorbed on the surface, was examined using confocal laser scanning microscopy. U2Os cells were cultured in DMEM medium at 37° C under a 5% atmosphere of CO_2. A suspention containing 100 µg/mL of FAMSNs in DMEM were incubated with U2Os cells for one hour. The cells were washed with 1 mL of PBS/EDTA for 2 min and then with 1 mL of PBS for other 2 min. Next, the cells were trypsonized with 1 mL of a 5% solution of trypsin for 10 min at 37° C. Cells were harvested with DMEM and centrifuged to remove any residual amount of trypsin which could affect the results of the experiment. Therefore the cells were resuspended in DMEM and the suspension was analyzed using flow cytometry. The several washing steps ensures that particles that adhered to the outer membrane surface, if any, were removed.

Quantification of nanoparticle uptake into U2Os cancer cells. To quantify the amount of nanoparticles included within the cells, U2Os cells were cultured in DMEM overnight in a lab-Teck chamber slide. The experiment was performed in triplo and the results shown are the average calculated from the obtained results. 1 mL of a suspention containing 1 µg mL^{-1} of FAMSNs in DMEM was added in each well of a 4 well Lab-Teck chamber slide. 12 wells of cancer cells were prepared with the above mentioned amount of FAMSNs in the medium, and every 2 hours 3 wells were harvested via trypsinization. The number of positive cells was determined with flow cytometry. In control experiments unmodified silica nanoparticles were used in order to compare the difference in cellular uptake.

TUNEL Staining assay. The TUNEL staining assay was performed using Roche Diagnostics kit (number 11 684 795 910). U2Os cells were incubated with a suspension of 1 µg mL^{-1} FAMSNs in DMEM for 1 hour at 37 °C and then they were rinsed with new DMEM (2mL). The cells were fixated with 1 mL of 4% pFA for 20 min and then permeabilized for 2 min on ice with 500 µL of a solution containing 0.1% of Triton, 0.1% of sodium citrate in Milli-Q water. The cells were rinsed with PBS for 15 min (2x1 mL). Next, the U2Os cells were incubated with 100 µL of TUNEL staining solution for 1 hours at 37 °C. Before laser confocal imaging the cells were rinsed again with PBS (2x1 mL).

Western blot analysis. U2Os cancer cells were cultured overnight in a 6 well plate (Lab-Tek Nunc) at 37 °C with 5% of CO_2. The cells were exposed to CPT-loaded-FASNP for 1 hour and washed with 1 mL of DMEM to remove the particles which were not taken up by the cells. Next, the cultured cells were washed with 1 mL of PBS (pH=7.24) for 10 min and lysed with 500 µL of SDS Sample Buffer for 5 minutes. The cells were then scraped off the plate and transferred in a microcentrifuge tube and kept on ice.

The lysates sample were sonicated for 10-15 seconds to shear DNA and to reduce the viscosity; afterwards aliquots of 20 µL were taken and heated at 95-100 °C for 5 minutes and cooled on ice. The DNA pellet was separated by a microcentrifugation for 5 minutes at 13,000 rpm. Aliquots of 20 µL of the supernatant were loaded on SDS-page gel for analysis. The electrophoresis was performed in TBS for 90 minutes at 90 mV.

The proteins were transferred from the SDS-gel to nitrocellulose membranes and rinsed with 25 mL of TBS buffer for 5 minutes at room temperature. The membranes were incubated with 20 mL of blocking buffer for 1 hour at room temperature and then washed with 15 mL of TBS-T (3x5 min). The incubation of the membranes with primary antibody (dilution 1:2000) was done overnight at 4 °C. Next, the nitrocellulose membranes were washed with 15 mL of TBS-T (3x5 min), and they have been incubated for 1 hour at room temperature with HRP-conjugated secondary antibody (dilution 1:2000) and HRP-conjugated anti-biotin antibody (dilution 1:1000) in 10 mL of blocking buffer.

The membranes were incubated with 10 mL of LumiGlo (0.5 ml of 20X LumiGlo, 0.5 mL 20X Peroxide and 9.0 mL of MilliQ water) with gentle agitation for 1 minute at room temperature. The membranes were taken out of the solution, wrapped in plastic paper, and exposed to X-ray film.

3.5 References and Notes

1. Asadishad, B.; Vosoughi, M.; Alamzadeh, I.; Tavakoli, A., Synthesis of Folate-Modified, Polyethylene Glycol-Functionalized Gold Nanoparticles for Targeted Drug Delivery. *Journal of Dispersion Science and Technology* **2010**, *31* (4), 492-500.
2. Vivero-Escoto, J. L.; Slowing, II; Trewyn, B. G.; Lin, V. S. Y., Mesoporous Silica Nanoparticles for Intracellular Controlled Drug Delivery. *Small* **2010***, 6* (18), 1952-1967.
3. Farokhzad, O. C.; Jon, S. Y.; Khademhosseini, A.; Tran, T. N. T.; LaVan, D. A.; Langer, R., Nanopartide-aptamer bioconjugates: A new approach for targeting prostate cancer cells. *Cancer Research* **2004,** *64* (21), 7668-7672.
4. Slowing, II; Trewyn, B. G.; Giri, S.; Lin, V. S. Y., Mesoporous silica nanoparticles for drug delivery and biosensing applications. *Advanced Functional Materials* **2007,** *17* (8), 1225-1236.
5. Boas, U.; Heegaard, P. M. H., Dendrimers in drug research. *Chemical Society Reviews* **2004,** *33* (1), 43-63.
6. Haag, R.; Kratz, F., Polymer therapeutics: Concepts and applications. *Angewandte Chemie-International Edition* **2006,** *45* (8), 1198-1215.
7. De Jong, W. H.; Borm, P. J. A., Drug delivery and nanoparticles: Applications and hazards. *International Journal of Nanomedicine* **2008,** *3* (2), 133-149.
8. Soussan, E.; Cassel, S.; Blanzat, M.; Rico-Lattes, I., Drug Delivery by Soft Matter: Matrix and Vesicular Carriers. *Angewandte Chemie-International Edition* **2009,** *48* (2), 274-288.
9. Torchilin, V. P., Lipid-core micelles for targeted drug delivery. *Current Drug Delivery* **2005,** *2* (4), 319-327.
10. Torchilin, V. P., Liposomal delivery of protein and peptide drugs. *Biomaterials for Delivery and Targeting of Proteins and Nucleic Acids* **2005**, 433-459.
11. Rosenholm, J. M.; Sahlgren, C.; Linden, M., Towards multifunctional, targeted drug delivery systems using mesoporous silica nanoparticles - opportunities & challenges. *Nanoscale* **2010***, 2* (10), 1870-1883.
12. Vallet-Regi, M.; Ramila, A.; del Real, R. P.; Perez-Pariente, J., A new property of MCM-41: Drug delivery system. *Chemistry of Materials* **2001,** *13* (2), 308-311.
13. Lu, J.; Liong, M.; Li, Z. X.; Zink, J. I.; Tamanoi, F., Biocompatibility, Biodistribution, and Drug-Delivery Efficiency of Mesoporous Silica Nanoparticles for Cancer Therapy in Animals. *Small* **2010***, 6* (16), 1794-1805.
14. Lu, J.; Liong, M.; Zink, J. I.; Tamanoi, F., Mesoporous silica nanoparticles as a delivery system for hydrophobic anticancer drugs. *Small* **2007,** *3* (8), 1341-1346.
15. Ambrogio, M. W.; Thomas, C. R.; Zhao, Y.-L.; Zink, J. I.; Stoddart, J. F., Mechanized Silica Nanoparticles: A New Frontier in Theranostic Nanomedicine. *Accounts of Chemical Research* **2011,** *44* (10), 903-913.
16. Nguyen, T. D.; Leung, K. C. F.; Liong, M.; Pentecost, C. D.; Stoddart, J. F.; Zink, J. I., Construction of a pH-driven supramolecular nanovalve. *Organic Letters* **2006,** *8* (15), 3363-3366.
17. Meng, H. A.; Liong, M.; Xia, T. A.; Li, Z. X.; Ji, Z. X.; Zink, J. I.; Nel, A. E., Engineered Design of Mesoporous Silica Nanoparticles to Deliver Doxorubicin and P-Glycoprotein siRNA to Overcome Drug Resistance in a Cancer Cell Line. *Acs Nano* **2011***, 4* (8), 4539-4550.
18. Ruiz-Hernandez, E.; Baeza, A.; Vallet-Regi, M., Smart Drug Delivery through DNA/Magnetic Nanoparticle Gates. *Acs Nano* **2011***, 5* (2), 1259-1266.
19. Lu, J.; Choi, E.; Tamanoi, F.; Zink, J. I., Light-activated nanoimpeller-controlled drug release in cancer cells. *Small* **2008,** *4* (4), 421-426.
20. Patel, K.; Angelos, S.; Dichtel, W. R.; Coskun, A.; Yang, Y. W.; Zink, J. I.; Stoddart, J. F., Enzyme-responsive snap-top covered silica nanocontainers. *Journal of the American Chemical Society* **2008,** *130* (8), 2382-2383.
21. Porta, F.; Lamers, G. E. M.; Zink, J. I.; Kros, A., Peptide modified mesoporous silica nanocontainers. *Physical Chemistry Chemical Physics* **2011***, 13* (21), 9982-9985.
22. Radu, D. R.; Lai, C.-Y.; Wiench, J. W.; Pruski, M.; Lin, V. S. Y., Gatekeeping Layer Effect: A Poly(lactic acid)-coated Mesoporous Silica Nanosphere-Based Fluorescence Probe for Detection of Amino-Containing Neurotransmitters. *Journal of the American Chemical Society* **2004,** *126* (6), 1640-1641.
23. Liu, R.; Zhang, Y.; Feng, P., Multiresponsive Supramolecular Nanogated Ensembles. *Journal of the American Chemical Society* **2009,** *131* (42), 15128-15129.
24. Low, P. S.; Kularatne, S. A., Folate-targeted therapeutic and imaging agents for cancer. *Current Opinion in Chemical Biology* **2009,** *13* (3), 256-262.
25. Sudimack, J.; Lee, R. J., Targeted drug delivery via the folate receptor. *Advanced Drug Delivery Reviews* **2000,** *41* (2), 147-162.

26. Hayashi, K.; Moriya, M.; Sakamoto, W.; Yogo, T., Chemoselective Synthesis of Folic Acid-Functionalized Magnetite Nanoparticles via Click Chemistry for Magnetic Hyperthermia. *Chemistry of Materials* **2009,** *21* (7), 1318-1325.
27. Liong, M.; Lu, J.; Kovochich, M.; Xia, T.; Ruehm, S. G.; Nel, A. E.; Tamanoi, F.; Zink, J. I., Multifunctional inorganic nanoparticles for imaging, targeting, and drug delivery. *Acs Nano* **2008,** *2* (5), 889-896.
28. Garcia-Bennett, A.; Nees, M.; Fadeel, B., In search of the Holy Grail: Folate-targeted nanoparticles for cancer therapy. *Biochemical Pharmacology* **2011***, 81* (8), 976-984.
29. Oh, J. M.; Choi, S. J.; Lee, G. E.; Han, S. H.; Choy, J. H., Inorganic Drug-Delivery Nanovehicle Conjugated with Cancer-Cell-Specific Ligand. *Advanced Functional Materials* **2009,** *19* (10), 1617-1624.
30. Gu, J.; Fan, W.; Shimojima, A.; Okubo, T., Organic-inorganic mesoporous nanocarriers, integrated with biogenic ligands. *Small* **2007,** *3* (10), 1740-1744.
31. Sun, L.; Zang, Y.; Sun, M. D.; Wang, H. G.; Zhu, X. J.; Xu, S. F.; Yang, Q. B.; Li, Y. X.; Shan, Y. M., Synthesis of magnetic and fluorescent multifunctional hollow silica nanocomposites for live cell imaging. *Journal of Colloid and Interface Science* **2010***, 350* (1), 90-98.
32. Wang, Z. Y.; Zong, S. F.; Yang, J.; Li, J.; Cui, Y. P., Dual-mode probe based on mesoporous silica coated gold nanorods for targeting cancer cells. *Biosensors & Bioelectronics* **2011***, 26* (6), 2883-2889.
33. Lai, C. Y.; Trewyn, B. G.; Jeftinija, D. M.; Jeftinija, K.; Xu, S.; Jeftinija, S.; Lin, V. S. Y., A mesoporous silica nanosphere-based carrier system with chemically removable CdS nanoparticle caps for stimuli-responsive controlled release of neurotransmitters and drug molecules. *Journal of the American Chemical Society* **2003**, *125* (15), 4451-4459.
34. Huh, S.; Wiench, J. W.; Trewyn, B. G.; Song, S.; Pruski, M.; Lin, V. S. Y., Tuning of particle morphology and pore properties in mesoporous silicas with multiple organic functional groups. *Chemical Communications* **2003**, (18), 2364-2365.
35. Slowing, II; Wu, C. W.; Vivero-Escoto, J. L.; Lin, V. S. Y., Mesoporous Silica Nanoparticles for Reducing Hemolytic Activity Towards Mammalian Red Blood Cells. *Small* **2009**, *5* (1), 57-62.
36. Hayashi, K.; Ono, K.; Suzuki, H.; Sawada, M.; Moriya, M.; Sakamoto, W.; Yogo, T., One-Pot Biofunctionalization of Magnetic Nanoparticles via Thiol-Ene Click Reaction for Magnetic Hyperthermia and Magnetic Resonance Imaging. *Chemistry of Materials* **2011***, 22* (12), 3768-3772.
37. Bose, A. K.; Ghoshmazumdar, B. N.; Chatterjee, B. G., Ease of cyclization to the beta-lactam ring. *Journal of the American Chemical Society* **1960,** *82* (9), 2382-2386.
38. Sheehan, J. C.; Bose, A. K., The synthesis and reactions of some substituted beta-lactams. *Journal of the American Chemical Society* **1951,** *73* (4), 1761-1765.
39. Cauda, V.; Argyo, C.; Bein, T., Impact of different PEGylation patterns on the long-term bio-stability of colloidal mesoporous silica nanoparticles. *Journal of Materials Chemistry* **2010***, 20* (39), 8693-8699.
40. Cauda, V.; Schlossbauer, A.; Bein, T., Bio-degradation study of colloidal mesoporous silica nanoparticles: Effect of surface functionalization with organo-silanes and poly(ethylene glycol). *Microporous and Mesoporous Materials* **2010***, 132* (1-2), 60-71.
41. Blumen, S. R.; Cheng, K.; Ramos-Nino, M. E.; Taatjes, D. J.; Weiss, D. J.; Landry, C. C.; Mossman, B. T., Unique uptake of acid-prepared mesoporous spheres by lung epithelial and mesothelioma cells. *American Journal of Respiratory Cell and Molecular Biology* **2007,** *36* (3), 333-342.
42. Elnakat, H.; Ratnam, M., Distribution, functionality and gene regulation of folate receptor isoforms: implications in targeted therapy. *Advanced Drug Delivery Reviews* **2004,** *56* (8), 1067-1084.
43. Elnakat, H.; Ratnam, M., Role of folate receptor genes in reproduction and related cancers. *Frontiers in Bioscience* **2006,** *11*, 506-519.
44. Bozard, B. R.; Ganapathy, P. S.; Duplantier, J.; Mysona, B.; Ha, Y.; Roon, P.; Smith, R.; Goldman, I. D.; Prasad, P.; Martin, P. M.; Ganapathy, V.; Smith, S. B., Molecular and Biochemical Characterization of Folate Transport Proteins in Retinal Muller Cells. *Investigative Ophthalmology & Visual Science* **2011***, 51* (6), 3226-3235.
45. Hashimoto, T.; Kikkawa, U.; Kamada, S., Contribution of Caspase(s) to the Cell Cycle Regulation at Mitotic Phase. *Plos One* **2011***, 6* (3).
46. Frank, A. K.; Pietsch, E. C.; Dumont, P.; Tao, J.; Murphy, M. E., Wild-type and mutant p53 proteins interact with mitochondrial caspase-3. *Cancer Biology & Therapy* **2011***, 11* (8), 740-745.
47. Bensasson, S. A.; Sherman, Y.; Gavrieli, Y., Identification of dying cells-in-situ staining. *Methods in Cell Biology, Vol 46* **1995,** *46*, 29-39.
48. Gavrieli, Y.; Sherman, Y.; Bensasson, S. A., identification of programmed cell-death in situ via specific labeling of nuclear-DNA fragmentation. *Journal of Cell Biology* **1992,** *119* (3), 493-501.

49. Wagner, V.; Dullaart, A.; Bock, A. K.; Zweck, A., The emerging nanomedicine landscape. *Nature Biotechnology* **2006,** *24* (10), 1211-1217.